International Journal of Thermophysics, Vol. 26, No. 4, July 2005 (© 2005)
DOI: 10.1007/s10765-005-6686-8

Thermodynamics of Refractory Nuclear Materials Studied by Mass Spectrometry of Laser-Produced Vapors[1]

R. Pflieger,[2] M. Sheindlin,[2,3] and J.-Y. Colle[2]

A new method of high-temperature mass spectrometry (MS) with laser-induced vaporization (LIV) has been developed. The initial problem of LIV MS, consisting of an inadequate correlation between the temperature of the surface and the MS signal, was successfully overcome.The method was developed on graphite, of which fast time-resolved MS measurements (ca. 20 ms) were performed over a large mass interval; the influence of geometrical parameters and of the laser pulse length on MS measurements was studied. Carbon sublimation relative partial pressures of C_1, C_2, C_3, and C_5 were measured up to 3810 K. This corresponds to a total pressure of about 0.8 bar estimated independently by the integral mass flux using the Hertz–Knudsen equation. The vaporization of UO_2 was studied at temperatures above $\approx$2500 K, where conventional Knudsen-cell mass spectrometry cannot be applied. The vaporization enthalpy obtained for the main species in UO_2 vapor was in good agreement with that of conventional mass spectrometry.

KEY WORDS: graphite; high temperature mass spectrometry; UO_2; vapor partial pressures.

1. INTRODUCTION

Evaluation of the sublimation/evaporation behavior of refractory materials at very high temperatures requires data on the equilibrium partial pressures of the vaporizing species. In particular, vaporization pressure data on

[1] Paper presented at the Seventh International Workshop on Subsecond Thermophysics, October 6–8, 2004, Orléans, France.

[2] European Commission, Joint Research Centre, European Institute for Transuranium Elements, Postfach 2340, D 76125 Karlsruhe, Germany.

[3] To whom correspondence should be addressed. E-mail: michael.sheindlin@itu.fzk.de

nuclear fuel materials are especially required to analyze hypothetical accident conditions and to carry out risk assessments.

Laser-induced vaporization (LIV) has been applied previously in order to extend the temperature and pressure ranges accessible for conventional high-temperature mass spectrometry. The first experiments date back to the late 1960s when because of the progress in laser technology laser energies became sufficient to reach temperatures at which vapor pressures, controlled by vaporization kinetics in vacuum, were approaching *ca.* 10 bar. Therefore, the composition of these high-temperature vapors could be analyzed by mass spectrometry. Obviously, due to the "pulsed" nature of this vaporization, several limitations were imposed on the mass spectrometric measurements. This is why in most of the previous investigations either time-integral measurements of the mass spectrum or only single mass time-resolved measurements have been performed due to the short heating time. Sufficiently accurate temperature measurements always constituted a problem for the same reason. Therefore, the temperature at the evaporating surface was, usually, calculated using one of the suitable evaporation models, the choice of which was often not sufficiently reliable. Some details of the previous studies are presented in Table I.

2. EXPERIMENTAL

The apparatus used in the present study was developed with the aim to overcome most of the above-mentioned difficulties and to increase the reliability of the measurements. The latter mostly concerns the regime of evaporation and, in particular, the issue of thermodynamic equilibrium at the evaporating surface.

Evidently, the main feature of a time-of-flight (TOF) mass spectrometer – the high speed of measurements – makes it the most promising tool for the high-speed mass spectra sampling of the laser-induced vapors. Although the repetition rate of TOF measurements is high, it cannot greatly exceed 50 kHz due to the flight time in the *ca.* 1 m long TOF flight tube. It means that one-millisecond pulse heating by the most conventional free-running solid-state lasers (not to mention nanosecond pulse heating) does not allow reliable time-resolved measurements by the TOF mass spectrometer.

Therefore, an ≈ 10 ms time length laser-heating pulse was implemented allowing several hundreds of mass spectra to be recorded. The temperature measurements are made along with the TOF spectra by high-speed pyrometry.

A schematic of the experimental apparatus is shown in Fig. 1. The laser evaporation is performed in a vacuum chamber, attached to the TOF

Table I. Summary of Laser-Heating Mass Spectrometric Studies

Reference	Year of publication	Material	Temperature	Mass spectrometer	Laser power density ($W \cdot cm^{-2}$)	Pressure range (bar)	Ionization method	Laser pulse	Averaging of the signal
Zavitsanos [1]	1968	graphite (**C**)	Calculated $\sim 4060-4100$ K	TOF MS	10^5–10^6	–	Electron Impact (EI)	0.5 ms	1 exp = 1 spectrum
Lincoln *et al.* [2]	1975	C (+Al_2O_3 and SiO_2)	Calculated $\sim 3200-4200$ K	TOF MS	–	–	EI	1/2–1/3 ms	
Olander *et al.* [3]	1988	UO_2 (+MgO+ZrO_2)	Measured ~ 1900–4200 K (fast pyrometer)	QMS	$(0.7 \text{ to } 4.5) \times 10^4$	$10^{-5}-10^2$	EI + Laser Ionization (LI)	0.45 or 1.1 ms	–
Joseph *et al.* [4]	1996	UO_2	Calculated 4300 K	QMS	$\sim 10^8$	3.9	LI	10 ns	over 100–1000 shots
Hastie *et al.* [5]	2001	C,ZrO_2, Y_2O_3, HfO_2	Measured (single, time-integrated spectroscopy) 3000–5000 K	QMS	4×10^7	0.01–20	EI	7–30 ns	–
Joseph *et al.* [6]	2002	UO_2, UC, ThO_2	Calculated 4700 and 5700 K	QMS	4.8×10^7 and 8.6×10^7	9.7 and 117	EI	8 ns	over 100–1000 shots
Joseph *et al.* [7]	2002	C	Calculated 4100–7100 K	QMS	$\leqslant 2 \times 10^8$	1 to 562	EI	8 ns	over 1000 shots

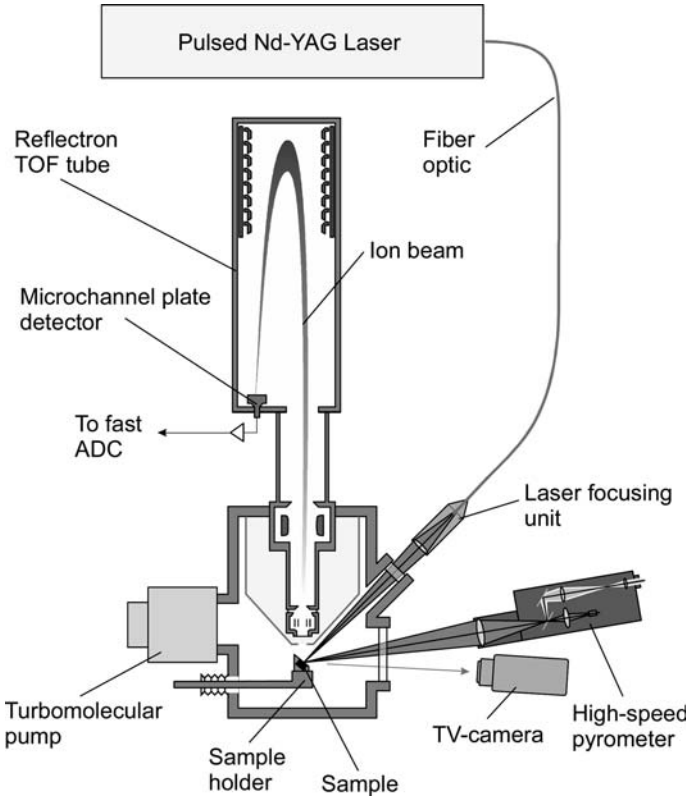

Fig. 1. Schematic of the experimental apparatus.

mass spectrometer, where a vacuum of 10^{-7} mbar is maintained. The sample is placed in a sample holder providing the several fixed angles formed by the sample surface and the axis of the mass spectrometer: 20, 30, 45, or 55°. The sample vacuum chamber is separated from the TOF mass spectrometer by a wall in such a way that the vapor molecules can enter the electron impact ionization source of the TOF mass spectrometer through a small hole in the skimmer fixed in the wall. The ions pushed out from the ionization chamber by a voltage pulse are separated in the flight tube of the TOF mass spectrometer according to their mass-to-charge ratio, and then detected by a multi-channel plate detector. The surface temperature is measured along with mass spectra by a high-speed brightness pyrometer.

2.1. Samples

Two materials were studied: carbon (in the form of graphite) and uranium dioxide. Both materials are of great technological importance and, therefore, their high-temperature properties (in particular, their high-temperature vaporization, see Table I) have already been extensively studied. In addition, their vaporization temperature levels are not very far from each other: at 1 bar the sublimation temperature of graphite is 4000 K and the boiling temperature of UO_2 is 3800 K.

Graphite was used in the preliminary study since it does not melt at the conditions of laser heating in vacuum under "moderate" laser power densities not exceeding $10^6\,W\cdot cm^{-2}$. It has very good mechanical stability at high temperature, and it does not form cracks even at high temperature gradients in the vicinity of the laser spot. Moreover, the available literature data on the vaporization thermodynamics of different carbon species seem to be quite reliable [8–10].

Pellets of 10 mm in diameter and 2–2.5 mm in thickness were cut out of a plate of pyrolytic graphite because of its high density ($2.16\,g\cdot cm^{-3}$) and highly anisotropic structure. The latter was used to improve the heating regime; since the thermal conductivity in the c-direction (depth) is small, less power density is required to achieve the needed temperatures. Mass spectra of this material showed that it contains some amounts of C_2H_2 and very little C_4H_2, with a total partial pressure that was estimated to be less than 1% of the total pressure.

Commercial nuclear grade UO_2 in the form of pellets of 8.35 mm in diameter and 12 mm length, fabricated by Advanced Nuclear Materials Co., was used. The stoichiometry of the pellets was $UO_{2.00\pm0.01}$. The 3–3.5 mm thick samples were cut with a low-speed diamond saw and cleaned successively in ethanol and acetone.

2.2. Laser Heating

A Nd:YAG laser of LASAG operating in the free-running mode is used. Its wavelength is 1064 nm, which is absorbed neither by carbon nor by UO_2 vapors. Laser pulses in the range of 18–20 ms were used. In any case laser power densities were below $2\times10^5\,W\cdot cm^{-2}$, preventing any risk of plasma formation. Since the laser beam is delivered to the focusing unit through an optical fiber, its radial power profile is very homogeneous at the exit of the fiber, which insures very high power homogeneity in the focal spot.

2.3. Temperature Measurements

The temperature is measured with a special high-speed brightness pyrometer. This pyrometer consists of focusing optics, a band-pass filter centered at 650 nm, and a Si-photodiode connected to a very high-speed logarithmic amplifier. Since none of the carbon/UO_2 vapor components absorbs at 650 nm, and since no ions are produced at the relatively low power densities used in these experiments, one can consider the vapor to be transparent at the used wavelength. The pyrometer is calibrated against a reference tungsten strip lamp. The literature values of emissivities were used for the conversion from brightness temperature to the true temperature: 0.88 for graphite [11] and 0.835 for UO_2 [12].

Due to the nature of the pyrometer with a logarithmic amplifier, the response speed of the pyrometer (amounted to 10 μs at temperatures higher than 2500 K) is sharply decreasing with a decrease in temperature. Since the temperature range for UO_2 was lower than that of graphite, the pyrometer could not always follow the temperature increase. To make it faster, the pyrometer has been modified in the following way: its detector is pre-lightened with a light-emitting diode (LED) generating a "virtual" temperature of 1960 K. During the measurement, the diode circuit opens automatically when the output signal reaches the value that corresponds to a real temperature of 2050 K. Then the measured signal is not modified anymore by the presence of the diode and corresponds to the real sample temperature.

2.4. Mass Spectrometer (MS)

A Reflectron time-of-flight (TOF) mass spectrometer is utilized, which allows simultaneous measurement of the signal intensities of all the vapor species in one experiment. After having passed the skimmer, molecules are ionized by electron impact during 500 ns; the energy of the electrons can be fixed between 4 and 120 eV. Then, after 100 ns, ions are subjected to a high acceleration voltage (1.5 kV) pulse of 100 ns and enter the flight tube. The time diagram is presented in Fig. 2.

The maximum repetition rate of the TOF MS depends on the maximum mass number to be measured: the repetition rate can be up to 50 kHz for graphite but not higher than 30 kHz for UO_2 (a higher repetition rate would cause overlapping of high masses of spectrum n with low masses of spectrum $n+1$).

Spectra are recorded every 20 or 33 μs during a heating pulse of approximately 20 ms. The setting of the mass range to a reasonably narrow interval was defined by the data acquisition. Since half-width times of the

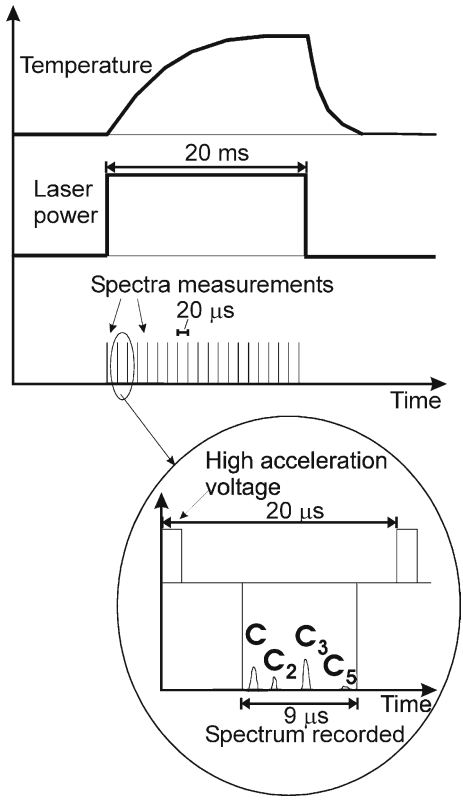

Fig. 2. Profiles of the temperature, the laser power, and the measured spectra as a function of time.

mass peaks are in the range of 5 to 10 ns, an ultra-fast data acquisition system with 8-bit ADC and 2 GHz sampling rate is used. As data have to be recorded even in the "dead interval" – between the mass peaks, the capacity of the buffer used (16 MB in this case) limits the mass interval. Concerning evaporation of graphite only, molecular species in the range of C_1 to C_5 were considered since larger molecules could not be detected in the preliminary experiments up to the highest attainable temperatures, and their amounts were negligible according to available thermodynamic predictions [8–10]. As for fullerenes and, in particular, C_{60} molecules, not all conditions of their formation are well known; in particular, the question still exists whether they are part of the equilibrium carbon vapor. To test the presence of C_{60} molecules in the vapor produced under the present

working conditions, the studied mass range was focused around m/z of 720. No peak could be seen. The intensity of C_5 as a function of temperature was determined in order to estimate the limit of quantification. This pentamer is visible starting from 3350 K. At this temperature, IVTANTHERMO thermodynamic tables give a C_3/C_5 ratio of 22. According to the experimental C_3/C_5 ratios (of the order of 15), one can consider to a first approximation that the vaporization coefficients of these two species are equal. Assuming that the vaporization coefficient of C_{60} is of this order or higher, one finds that the partial pressure of C_{60} at 3350 K is at most 22 times less than that of C_3. Finally, the C_4 presence is only qualitatively detected (indeed, according to available thermodynamic predictions, its amount is around six times less than that of C_5 in the temperature interval 3200–3800 K). The flight time of C_1 is approx. 7100 ns, and that of C_5 is 15700 ns. The resulting length of the spectrum is, therefore, about 9000 ns each, stored in one of the max. 8000 sub-buffers.

The primary data analysis consists of the correction for background, definition of the mass peaks, and calculation of their areas that gives the values of the intensities.

In order to get intensities and temperatures that are related and correspond to the hot spot of the sample surface, the TOF MS, laser, and pyrometer are carefully adjusted before each experiment, so that their axes are crossing at one point on the sample surface. A small pilot diode laser beam is entering the mass spectrometer and redirected by a prism to be in line with the axis of the TOF MS. This pilot beam is passing through a small hole in the skimmer giving a reference position for the laser spot of 2 mm in diameter. The optical pyrometer (having a sighting spot of 0.5 mm) is focused in the center of the laser spot. This procedure insures the reproducibility of experimental conditions.

As for the calibration of the mass scale of the mass spectrometer and of the cathode voltage used for the electron energy calculation, it is performed using a mixture of rare gases in nitrogen with known appearance potentials.

2.5. Measurement of Crater Depth by Profilometry

In order to estimate the total pressure, the depth of the formed craters, related to the total quantity of vaporized material, is measured by profilometry (Hommelwerke, Hommel Tester T10 G-2). The sensitivity value, given by calibration, is 0.1 μm on the vertical scale. The surface of the sample to be analyzed is swept by a continuous longitudinal movement of the sensor, after what the sample is slightly displaced for a new sweeping.

2.6. Calculation of the Partial Pressures

Mass intensity ratios, $I(C_n)/I(C_1)$, at a given temperature are converted into partial pressure ratios using the formula of Meyer and Lynch [13];

$$\frac{p(C_n)}{p(C_1)} = \frac{I(C_n)}{I(C_1)} \times \frac{\sigma(C_1)}{\sigma(C_n)} \times \frac{\Delta E(C_1)}{\Delta E(C_n)} \times \frac{\gamma(C_1)}{\gamma(C_n)} \times \frac{\beta(C_1)}{\beta(C_n)}. \tag{1}$$

The conversion factors consist of ratios of maximum ionization cross sections σ, ionization cross sections at the energy of the ionizing electrons relative to the maximum ionization cross sections ΔE, secondary electron yields of the electron multiplier γ, and spectrometer transmission coefficients β.

For the ionization cross sections, the "modified" ionization cross-section formula derived empirically by Palmer and Shelef [14] was used;

$$\sigma(C_n)/\sigma(C_1) = (1.5)^{n/2} \quad (\text{for } n > 1). \tag{2}$$

Taking C_1 as a reference, the following relative ionization cross sections are obtained: $\sigma(C_2) = 1.50$, $\sigma(C_3) = 1.84$, and $\sigma(C_5) = 2.76$.

The secondary electron yields of the electron multiplier were calculated according to Meyer and Lynch [13], upon inverse square root of mass dependence of secondary electron yield, assuming a value of one for C_1: $\gamma(C_2) = 0.71$, $\gamma(C_3) = 0.58$, and $\gamma(C_5) = 0.45$.

Relative ionization coefficients were defined as

$$\frac{\Delta E(C_n)}{\Delta E(C_1)} = \frac{E - \mathrm{AP}(C_n)}{E - \mathrm{AP}(C_1)}, \tag{3}$$

where E is the energy of the ionizing electrons and AP is the appearance potential of the ion. The appearance potentials reported by Drowart *et al.* [15] were used: $\mathrm{AP}(C_1) = 11.3$ eV, $\mathrm{AP}(C_2) = 12.0$ eV, $\mathrm{AP}(C_3) = 12.6$ eV, and $\mathrm{AP}(C_5) = 12.5$ eV.

As for the transmission coefficients, they were assumed to be equal for the given experimental conditions.

Similar conversion factors were determined for the ratio of the partial pressures of UO_2 vapor species, using relative ionization cross sections recommended by Younès [16] ($\sigma(UO)/\sigma(UO_2) \times \Delta E(UO)/\Delta E(UO_2) = 1.45 \times 1.28$ at 13 eV).

3. RESULTS AND DISCUSSION

3.1. Graphite

3.1.1. Reproducibility

It was observed that the mass intensities depend on the state of the surface, i.e., on the number of repeated laser shots on the same point of the sample surface. Therefore, the reproducibility of the method was tested by comparing results of several first (resp., second or third) shots on graphite sample surfaces, each time using the same laser pulse length (20 ms) and the same angle of inclination to the axis of the MS. The partial vapor pressures measured at each laser shot were presented as Arrhenius plots: $\ln(I_n T)$ versus $1/T$ where the slope of the line depends on the sublimation enthalpy: $-\Delta H_s/R$. It was found that the vapor-pressure curves measured during first laser shots on the "fresh" surface are not reproducible. The results obtained in the second and third shots are similar and do not depend on the particular sample. Therefore, the results of first shots were always discarded in the study of graphite.

3.1.2. Sublimation Enthalpies

3.1.2.1 Influence of the Electron Energy on Ion Intensity Ratios. The evolution of the intensity ratios as a function of the electron energy was studied to verify that the studied molecules are not undergoing any fragmentation due to the ionizing electrons. The ratios C/C_2 and C/C_3 were determined at different electron energies, varied between 13 and 39 eV, as can be seen in Fig. 3. At very low energies (13 eV), the signals are too low. Then, whereas C/C_2 stays constant up to the highest electron energies, C/C_3 is constant between 16 and 20 eV, then increases, which corresponds to a fragmentation of C_3 in C and C_2. Therefore, an electron energy of 16 eV was chosen to ensure sufficiently high signal/noise ratio without any significant fragmentation. The latter has to be taken into account for the proper comparison with the previously published results on LIV mass spectrometry of carbon. Thus, an electron energy of 20 eV was employed by Zavitsanos [1], which ensured that no appreciable fragmentation could occur. However, Hastie [5] and Joseph [4] used, respectively, 26 and 28 eV, which is above the fragmentation threshold of C_3.

3.1.2.2. Shape of the Arrhenius Plots and Sublimation Enthalpies. Vaporization enthalpies are obtained by a linear fit of the Arrhenius plots (Fig. 4) of experimental partial pressures in the temperature interval of 3250–3850 K or somewhat smaller (depending on the heating speed and the sample inclination angle). The MS signal/noise ratio, for

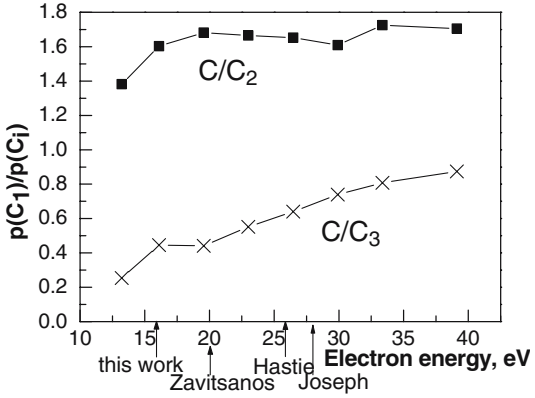

Fig. 3. Intensity ratios C/C_2 and C/C_3 as a function of the electron energy.

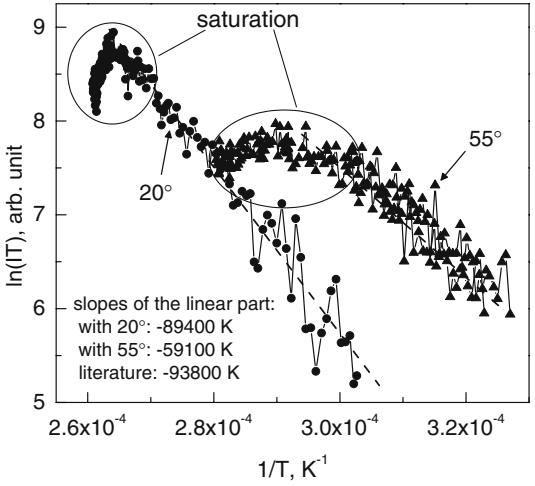

Fig. 4. Arrhenius plots obtained on graphite with 20 and 55°.

a small inclination angle (20°), at temperatures below 3250 K is too low. The upper limit of measurements (around 3750–3850 K) is defined by a saturation phenomenon; when the temperature is still ascending, the ion intensities decrease. This kind of behavior is caused by the expanded high-pressure vapor plume performing as a screen between the surface and the skimmer, reducing the molecular flux from the evaporating surface; vapor

Table II. Sublimation Enthalpies of C, C_2, C_3, and C_5, in $kJ \cdot mol^{-1}$: Literature [8, 9] and Experimental (with 20 or 30°) Values

Species	C	C_2	C_3	C_5
ΔH_s [8] ($T = 3000$ K)	711.9	812.4	797.4	1024
ΔH_s [8] ($T = 3000$ K)	707.3	802.1	779.5	1002
ΔH_s ([9])	708.9	823.5	832.6	1028
Experimental: 20°	677	621	782	–
Experimental: 30°	616	564	766	–

molecules cannot enter the skimmer without undergoing collisions in the vapor, so that the measured intensity is progressively attenuated.

The values of the sublimation enthalpies ΔH_s ($kJ \cdot mol^{-1}$) are given in Table II for C, C_2, C_3, and C_5 as calculated in IVTANTHERMO thermodynamic tables [8] at 3000 and 3700 K (note that the differences between the enthalpy values at both temperatures are very small) and values given by Leider *et al.* in [9]. Experimentally obtained enthalpy values are also presented in Table II; their uncertainty is about 2%. The intensity of C_5 is too low to allow an estimation of its sublimation enthalpy. One can see that the experimental results obtained at low angles are very close to the literature values for the three main species, indicating that there is a perfect correlation between the measured MS intensities and the surface temperatures. They do not show any appreciable dependence on the distance between the sample and the entrance of the mass spectrometer but on the angle between the surface and the axis of the mass spectrometer; too small enthalpies are obtained with larger angles. Indeed, the saturation phenomenon is more pronounced for large angles, for which the sample surface faces more the entrance of the mass spectrometer. The latter is confirmed by the study of the vapor curve dependence on the inclination angle, which was performed in the range of 20–55°. The mass intensity increases with an increase of the angle, as can be seen in Fig. 4, because the vapor plume develops mostly perpendicularly to the sample surface. As for the shape of the vaporization curve (which is supposed to be linear when presented as an Arrhenius plot), it is strongly curved for 55° angle, gives a more reasonable shape for 45° and, finally, approaches the literature values at 30°. As follows from Table II, a further decrease of the angle to 20° does not strongly affect the enthalpy values; however, the linear part of the vaporization line is extended towards higher temperatures. The bending point on the graph in Fig. 4 becomes sharper at the smallest angle and, therefore, defines data used for the linear regression more

precisely. Therefore, enthalpy values obtained for the inclination angle of 20° are closer to the thermodynamic calculations.

3.1.3. Vapor Pressures

3.1.3.1. Determination of the Appearance Potentials. The main vapor species C, C_2, C_3, and C_5 can be detected with sufficiently good accuracy under the conditions used here. Their appearance potentials were determined using a sample inclined at 20° at temperatures up to 3700 K. The electron energy was varied in the range of 13–19 eV. The corresponding intensities of the different carbon species were defined as the average intensities over the temperature interval from 3640 to 3660 K. Linear fits of these intensities versus the electron energy give the following appearance potentials: $AP(C_1) = 11.26$ eV, $AP(C_2) = 11.93$ eV, $AP(C_3) = 12.15$ eV, and $AP(C_5) = 10.41$ eV. The appearance potentials for C_1, C_2, and C_3 are in good agreement with values of Drowart *et al.* [15] (cf Section 2.6), and in acceptable agreement for C_5 due to its low intensity.

3.1.3.2. Relative Partial Pressures. The results obtained for the samples placed at 20° and 30° with a 16 eV ionization energy are given in Table III. All values are the averages taken in a temperature interval of 40 K centered on the indicated temperature. The indicated uncertainties are the standard deviations. For comparison, ratios calculated from the new version of IVTANTHERMO thermodynamic tables [8] are also presented in Table III.

With the intensity of C_5 being very low, the ratio C/C_5 has a large uncertainty and therefore gives only very rough information about the fraction of C_5 in carbon vapor at given temperatures.

Table III. Intensity Ratios Obtained with Samples at 20° and 30°, and Reference Values from IVTANTHERMO Thermodynamic Tables [8] at Different Temperatures

	Ratio	3450 K	3550 K	3650 K	3750 K
20°	C/C_2	1.25 ± 0.30	1.43 ± 0.26	1.30 ± 0.19	1.52 ± 0.13
	C/C_3	0.461 ± 0.075	0.502 ± 0.096	0.421 ± 0.061	0.376 ± 0.036
	C/C_5	11.6 ± 6.6	11.8 ± 3.0	18.1 ± 6.0	19.9 ± 3.7
30°	C/C_2	1.12 ± 0.36	1.15 ± 0.15	1.26 ± 0.18	1.48 ± 0.06
	C/C_3	0.468 ± 0.184	0.398 ± 0.049	0.378 ± 0.051	0.323 ± 0.051
	C/C_5	15.2 ± 5.3	14.6 ± 4.0	17.8 ± 4.9	19.5 ± 3.7
[8]	C/C_2	0.974	0.887	0.811	0.744
	C/C_3	0.106	0.0985	0.0919	0.0860
	C/C_5	1.82	1.35	1.02	0.777

Results obtained for the inclination angles of 20 and 30° are not significantly different. Taking the intensity of C as a reference, the concentration of C_2 agrees with the values of IVTANTHERMO thermodynamic tables [8] within 30% at 3450 K and within 100% at 3750 K. However, the measured concentration of C_3 appears to be *ca.* 5 times lower than thermodynamically predicted [8, 9]. Since C_3 and C are the major species in carbon vapor, the obtained disagreement is large and cannot be ignored. Here, one must make a remark that all the above discussion is made presuming that the evaporation is at equilibrium, which can be ensured only by minimization of the total vapor flux as is realized in Knudsen cells. Thus, the relative values, presented in Table III, were calculated assuming equilibrium evaporation. However, in the laser-induced evaporation the latter conditions cannot be achieved. Since relatively long laser pulses are applied and the laser power densities are rather low, a free surface (Langmuir type) evaporation was considered and, therefore, the deviation of vaporization coefficients from unity had to be taken into account.

The almost only available literature values determined by Burns *et al.* [17] in a Knudsen cell vaporization study were used: $\alpha_v(C) = 0.23 \pm 0.04, \alpha_v(C_2) = 0.38 \pm 0.04$, and $\alpha_v(C_3) = 0.04 \pm 0.005$. These coefficients were determined in Ref. 17 at 2500 K; however, they are considered to be independent of temperature. The corrected values of partial pressures are given in Table IV for 20° and 30°, together with values from the literature [8, 9, 14]. In Fig. 5, the partial pressure ratios $p(C_1)/p(C_3)$ are presented both before and after correction with vaporization coefficients. The corrected partial-pressure ratio shows very good agreement with equilib-

Table IV. Intensity Ratios at Different Temperatures, Corrected with Vaporization Coefficients (20° and 30° Angles and Reference Values [8, 9, 14], Values of Refs. 9 and 14 Obtained by Interpolation)

	Ratio	3450 K	3550 K	3650 K	3750,K
20°	C/C_2	2.06 ± 1.10	2.36 ± 1.13	2.14 ± 0.94	2.51 ± 0.95
	C/C_3	0.080 ± 0.038	0.087 ± 0.044	0.073 ± 0.034	0.065 ± 0.026
30°	C/C_2	1.85 ± 0.93	1.90 ± 0.79	2.51 ± 0.88	2.44 ± 0.78
	C/C_3	0.081 ± 0.056	0.069 ± 0.029	0.066 ± 0.028	0.056 ± 0.026
[8]	C/C_2	0.974	0.887	0.811	0.744
	C/C_3	0.106	0.0985	0.0919	0.0860
[9]	C/C_2	1.22	1.11	1.01	0.913
	C/C_3	0.096	0.089	0.082	0.074
[14]	C/C_2	1.7	1.5	1.3	1.1
	C/C_3	0.28	0.26	0.23	0.20

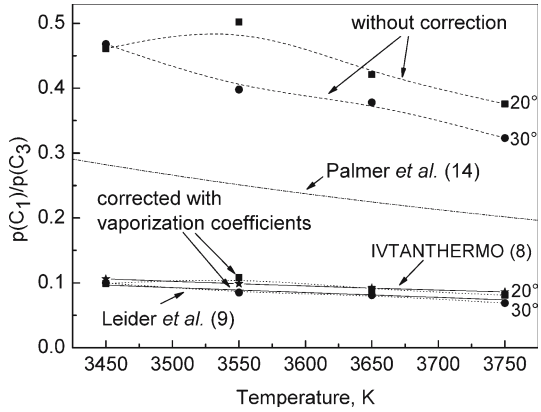

Fig. 5. Intensity ratios C/C_3 at different temperatures and a sample angle of 20 or 30°, corrected or not with vaporization coefficients and compared with literature values [8, 9, 14].

rium values, in spite of the uncertainties, mainly due to the uncertainty on the vaporization coefficients. The $p(C_1)/p(C_2)$ ratio reveals acceptable agreement with the various literature values, which also present some disagreement with each other. The larger uncertainty on this latter ratio is also due to the rather low C_2 intensity.

One can conclude that agreement of the relative partial pressures corrected with vaporization coefficients with those recommended in the literature confirm the assumption of Langmuir-type evaporation.

3.1.4. Estimation of the Total Pressure

The total carbon vapor pressure was estimated using the Hertz–Knudsen formula [18] assuming free molecular evaporation;

$$p_{\text{sat}} = \frac{\rho d}{\alpha_{\text{v}} \alpha_{\text{c}} \tau} \left(\frac{2\pi RT}{M} \right)^{1/2} \frac{1}{1-B}, \tag{4}$$

where p_{sat} is the total equilibrium vapor pressure, α_{v} is the integral vaporization coefficient of graphite, α_{c} is its condensation coefficient, ρ is the density of pyrolytic graphite, d is the crater depth, τ is the laser pulse length, R is the universal gas constant, T is the maximum surface temperature, M is the molar mass of the average molecule, and B is the total backscatter coefficient. For the integral vaporization coefficient of graphite, the value determined by Burns *et al.* [17] was taken: $\alpha_{\text{v}} = 0.07 \pm 0.04$. The condensation coefficient was taken as unity and the backscattering

Table V. Estimation of the Total Pressure via Crater Depth Measurement

Sample	Number of shots performed	$T_{max}(k)$	d_{max} (μm)	p (bar)	T(K)	p_{sat}[8] (bar)	p_{sat} [19] (bar)
1	6	3848 ± 15	150 ± 5	0.99	3810	0.50	0.44
2	6	3832 ± 15	130 ± 5	0.85	3830	0.59	0.50
3	6	3826 ± 10	116 ± 2	0.76	3850	0.70	0.56
4	6	3812 ± 11	140 ± 2	0.92			

coefficient as 0.18 (cf. Ref. 18). The measured room-temperature density of pyrolitic graphite is $\rho = 2.16 \pm 0.06\,\mathrm{g \cdot cm^{-3}}$. The chosen average degree of polymer formation is three, as given by Leider *et al.* [9] for temperatures around 3500 K, and so the average molar mass is $M = 36 \times 10^{-3}\,\mathrm{kg \cdot mol^{-1}}$.

The measurements of crater depths are made by profilometry. The measurement uncertainty is 0.05 μm for each measurement. The value of the maximum depth was taken since it corresponds to the center of the laser spot as viewed by a pyrometer.

The definition of the laser pulse length (τ) is not straightforward since the temperature is not constant during the laser shot. Its end point was taken as the end of the laser pulse and its beginning as the time at which the pressure is half of the maximum pressure reached during the shot. This gives $\tau = 10.6$ ms. It was calculated that the mass vaporized during the first 9.4 ms corresponds to only 15% of the total mass loss and is neglected here.

The obtained results are summarized in Table V that presents the maximum temperature reached, the corresponding crater depth, and the calculated total pressure.

These values are around 1.5 to 2 times higher than values given by IVTANTHERMO thermodynamic tables [8] and by the experimental equation given by Sheindlin [19]. However, the agreement is still good, considering the different assumptions made, especially regarding the value of the effective pulse length, τ and the large uncertainty on the integral vaporization coefficient.

3.2. Uranium Dioxide

One of the main problems in the study of UO_2 sublimation is the right choice of the electron energy. Indeed, according to Ref. 20, the ionization energies of the main species: UO, UO_2, and UO_3 are (in con-

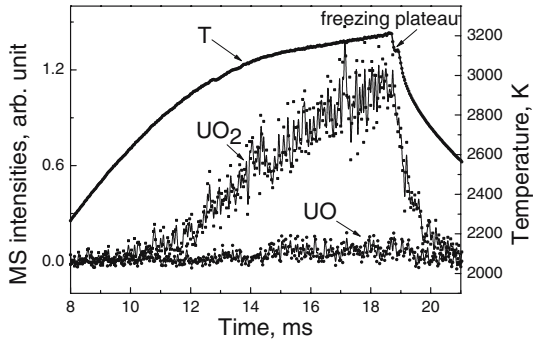

Fig. 6. Experimental thermogram and corresponding UO and UO_2 MS intensities during a 18-ms laser shot (during the first 8 ms of the laser shot, temperature and intensity are too low to be measured).

trary to carbon) quite different and amount, respectively, to 5.6, 5.4, and 10.8 eV. The noticeable fragmentation of UO_3 into UO_2^+ starts at 11.3 eV, of UO_3 in UO^+ at 19.3 eV, that of UO_2 in UO^+ at 13.4 eV, and of UO in U^+ at 13.9 eV. Therefore, the ionizing electron energy of 13 eV is used as it is sufficient for the ionization of the main species in the vapor and insures reasonably high ion signals. On the other hand, the degree of molecular fragmentation at this electron energy is negligible.

The main species experimentally observed was UO_2, followed by a small amount of UO and a tiny amount of UO_3 (which is less ionized at the working electron energy).

An example of a thermogram with the corresponding MS intensities of UO and UO_2 is given in Fig. 6. The chosen experimental conditions insured a continuous temperature increase during the whole duration of the laser shot (i.e., 18 ms). On the temperature descending flank of the thermogram, a short freezing "plateau" can be observed.

Experimental UO_2 Arrhenius plots are linear in the temperature interval of *ca.* 2500–3040 K. No saturation phenomenon was observed at these temperatures (this, however, is understandable since the maximum pressures reached here are much less than over graphite at 3850 K). Sublimation enthalpies were determined and compared with the one derived from UO_2 partial pressures measured by Ackermann *et al.* [21] between 1800 and 3100 K: 578.7 $kJ \cdot mol^{-1}$. It was found that the present enthalpy result was close to the literature value [21], giving 571 ± 58 $kJ \cdot mol^{-1}$ (as a mean value of four experiments).

The partial pressure ratios $p(UO_2)/p(UO)$ were calculated at 2930 ± 50 K and at 3040 ± 50 K giving, respectively, 20.1 ± 3.8 and 23.9 ± 4.7. These values are very far from the ratio calculated using the chemical equilibrium model [22] at 3000 K: 99.8, but in better agreement with the values obtained when considering a forced-congruent mode [22] (i.e., a vapor of average O/U ratio 2.00) at 3000 K: 11.9. The observed difference probably comes from the fragmentation of some UO_3 molecules into UO_2^+ at the used electron energy (fragmentation that increases the $p(UO_2)/p(UO)$ ratio). So, it seems that under these conditions, the vaporization can be considered as close to forced-congruent.

4. CONCLUSION

A new method of high-temperature mass spectrometry (MS) with laser-induced vaporization (LIV) was developed, in which the MS signals of various molecular species and the corresponding surface temperature are measured simultaneously.

The influence of geometrical parameters and of the laser pulse length on MS measurements was studied; it was found that the best operating conditions can be achieved at low inclination angles of the surface to the axis of the TOF MS and with a pulse length of less than 20 ms, because these conditions minimize saturation of the MS signal.

Carbon sublimation relative partial pressures of C_1, C_2, and C_3 were measured up to 3810 K. Thermodynamically sound relations between the partial pressures of the three main carbon vapor species were obtained using literature values of evaporation coefficients $\alpha_V(C_n)$. It confirms that the conditions of the experiment are very close to Langmuir evaporation.

Sublimation of UO_2 was studied at temperatures above 2500 K. In the vapor over stoichiometric uranium dioxide, mainly UO_2 but also UO and UO_3 molecules are seen under the present conditions. The sublimation enthalpy obtained for UO_2 from Arrhenius plots is in good agreement with results of conventional mass spectrometry.

ACKNOWLEDGMENTS

The authors would like to express their gratitude to C. Ronchi and L. Gorokhov for very fruitful discussions and suggestions, to J.-P. Hiernaut for practical advice, and to W. Heinz for his invaluable help in the setup of the equipment.

REFERENCES

1. P. D. Zavitsanos, *Carbon* **6**:731 (1968).
2. K. A. Lincoln and M. A. Covington, *Int. J. Mass Spectrom. Ion Phys*. **16**:191 (1975).
3. D. R. Olander, S. K. Yagnik, and C. H. Tsai, *J. Appl. Phys*. **64**:2680 (1988).
4. M. Joseph, N. Sivakumar, D. D. A. Raj, and C. K. Mathews, *Rapid Comm. Mass Spectrom*. **10**:5 (1996).
5. J. W. Hastie, D. W. Bonnell, and P. K. Schenck, *J. Nucl. Mat*. **294**:175 (2001).
6. M. Joseph, N. Sivakumar, and P. Manoravi, *High Temp.-High Press*. **34**:411 (2002).
7. M. Joseph, N. Sivakumar, and P. Manoravi, *Carbon* **40**:2031 (2002).
8. L. V. Gurvich, V. S. Iorish, D. V. Chekhovsioi, and V. S. Yungman, *NIST Special Database 5, "IVTANTHERMO"* (CRC, Boca Raton, Florida, 1993).
9. H. R. Leider, O. H. Krikorian, and D. A. Young, *Carbon* **11**:555 (1973).
10. M. W. Chase Jr., J. R. Downey Jr., D J. Frurip, R. A. McDonald, and A. N. Syvernd, eds., *JANAF Thermochemical Table*, 3rd edn. (American Institute of Physics, New York, 1985).
11. A. Basharin and M. Sheindlin, in "*Temperatura-84*," L'vov (1984), p. 49. [in Russian].
12. J. K. Fink, M. G. Chasanov, and L. Leibowitz, *ANL-CEN-RSD-80-4*, Argonne National Laboratory (April 1981).
13. R. T. Meyer and A. W. Lynch, *High Temp. Sci.* **5**:192 (1973).
14. H. B. Palmer and M. Shelef, *Chemistry and Physics of Carbon* 4, P. L. Walker, Jr., ed. (Marcel Dekker, New York, 1968), pp. 95–135.
15. J. Drowart, R. P. Burns, G. DeMaria, and M. G. Inghram, *J. Chem. Phys.* **31**:1131 (1959).
16. C. Younès, *Ph. D. Thesis* (Université Paris-Sud, Centre d'Orsay, Orsay, France, 1986), pp. 78–81.
17. R. P. Burns, A. J. Jason, and M. G. Inghram, *J. Chem. Phys.* **40**:1161 (1964).
18. J. Magill, C. Cercignani, and R. W. Ohse, *High Temp.-High Press.* **14**:441 (1982).
19. M. A. Sheindlin, *Int. J. Thermophys.* **13**:95 (1992).
20. F. Capone, J.-Y. Colle, J.-P. Hiernaut, and C. Ronchi, *J. Phys. Chem. A* **103**:10899 (1999).
21. R. J. Ackermann, E. G. Rauh, and M. H. Rand, *Symp. Thermodynamics of Nuclear Materials Julich 1979* **1**, IAEA:11, Vienna (1980).
22. C. Ronchi, I. L. Iosilevski, and E. Yakub, *Equation of State of Uranium Dioxide* (Springer-Verlag, Berlin, Heidelberg, 2004).